for NO_2 and CN, respectively, together with product, PhSeMe. The former peak was identified as 4-aminophenyl methyl selenide (lit.[27] 182.0 ppm) and the latter tentatively assigned to 4-aminomethylphenyl methyl selenide by using the σ value of aminomethyl (-0.22)[12] and the following equation:[27] $\delta(^{77}Se) = 202.6 + 32.5\sigma$ (calcd 199.0 ppm; found 194.8 ppm). Clearly these products are formed from the reduction of the substituents, a phenomenon that has previously been observed with thiophenoxide[28] and may cause the intense color of these solutions as noted above.

This competing reduction of starting material by $PhSe^-$ was of less significance in the rate studies because reaction times were of the order of a few minutes, due to the excess of methyl aryl selenide.

For X = NMe_2, where the equilibrium constant is far from unity, the product anion was not observed. The equilibrium constant was therefore obtained by using the following relationship: $K = x^2/(a - x)(b - x)$, where $a = [ArSeMe]_0$, $b = [PhSe^-Na^+]_0$, $x = ac/(1 + c)$, and c is given by eq 5.

$$c = \frac{[PhSeMe]_e}{[ArSeMe]_e} = \frac{^{77}Se \text{ peak ht of PhSeMe at equilibrium}}{^{77}Se \text{ peak ht of ArSeMe at equilibrium}} \quad (5)$$

(28) Porter, H. K. *Org. React.* **1973**, *20*, 455.

For all the remaining substituents, equilibrium constants were obtained directly from the ^{77}Se NMR spectra by using the expression

$$K = \frac{[ArSe^-]_e[PhSeMe]_e}{[PhSe^-]_e[ArSeMe]_e} = \frac{(^{77}Se \text{ peak ht of } ArSe^-_{eq})(^{77}Se \text{ peak ht of } PhSeMe_{eq})}{(^{77}Se \text{ peak hut of } PhSe^-_{eq})(^{77}Se \text{ peak ht of } ArSeMe_{eq})} \quad (6)$$

In all cases, errors in peak heights were obtained from the root mean square noise and these in turn were used to calculate the error in K. In one case, X = Me, the equilibrium mixture was analyzed by HPLC (using pre-prepared volumetric solutions to correct for the different extinction coefficient of ArSeMe and PhSeMe at 250 nm) and the mean value obtained: $K = 0.37$ is in excellent agreement with that given in Table I. In another example, X = Cl and F, the values were checked for internal consistency by determining the equilibrium constant between 4-fluorophenyl methyl selenide and the sodium salt of 4-chlorophenyl selenide (formed in situ from bis(*p*-chlorophenyl) diselenide). The value obtained, $K = 0.28$, is in breathtaking agreement with that obtained from Table I: $K(F)/K(Cl) = 2.45/8.5 = 0.29$.

For the X = CF_3 case, a similar relay procedure affords a value of $K(CF_3)/K(Cl) = 7.7$. Taking $K(Cl) = 8.5 \pm 2.5$ (Table I) affords a value of $K(CF_3) = 69 \pm 19$. This is the value quoted in Table I.

The Mechanism for the Conversion of α-Amino-β-carboxymuconate ϵ-Semialdehyde to Quinolinate, an Apparent Nonenzymic Step in the Biosynthesis of the Nicotinamide Coenzymes from Tryptophan[1]

Loren D. Keys, III, and Gordon A. Hamilton*

Contribution from the Department of Chemistry, The Pennsylvania State University, University Park, Pennsylvania 16802. *Received March 20, 1986*

Abstract: In the biosynthesis of the nicotinamide coenzymes from tryptophan in animals, apparently one step, namely, the conversion of α-amino-β-carboxymuconate ϵ-semialdehyde (**2**) to quinolinate (pyridine-2,3-dicarboxylate), proceeds by a nonenzyme-catalyzed reaction, even though it occurs at a branchpoint in typtophan metabolism. Because of its importance to mammalian metabolism, the mechanism of this nonenzymic reaction has been investigated and is reported here. In aqueous solution at 37 °C, quinolinate is the only product seen above pH 4.5, while below that pH a proton-catalyzed reaction forming α-hydroxymuconate semialdehyde competes with quinolinate formation. The pH rate profile for quinolinate formation consists of a plateau rate (near pH 4.5) which titrates (pK_a of **2** is 5.0) to a slower rate from ca. pH 7 to 11 and a hydroxide-catalyzed reaction at greater pH values. The reaction from pH 7 to 11 exhibits buffer catalysis and a change in rate-determining step. The zero buffer reaction occurs with a large solvent isotope effect ($k_{H_2O}/k_{D_2O} \geq 2.3$) and a secondary isotope effect ($k_D/k_H = 1.14$, D on aldehyde of **2**). Increasing the Tris buffer to 500 mM results in a loss of buffer catalysis, a loss of solvent deuterium isotope effect, and no change in secondary isotope effect. Catalysis by both the acidic and basic forms of the buffers is apparent. General acid catalysis is indicated by a Brønsted coefficient of $\alpha = 0.3$–0.4, and no catalytic advantage is seen with the catalysts dihydrogen phosphate and bicarbonate. These results indicate that carbinolamine dehydration is probably rate determining at low buffer concentrations while carbinolamine formation, probably by a pericyclic mechanism, is rate determining at high buffer concentrations. Under physiological conditions the reaction would be proceeding at a constant rate that would be insensitive to normal physiological fluctuations. Thus, control of this branchpoint in tryptophan metabolism is probably effected by control of the decarboxylase enzyme that competes with this nonenzymic step.

In animals, quinolinate (pyridine-2,3-dicarboxylate, **3**) and the nicotinate ring of the nicotinamide coenzymes are biosynthesized from tryptophan in a sequence of reactions outlined in abbreviated form in Scheme I.[2] That this is an important pathway in animal metabolism is evident from the observations that tryptophan can supply the entire niacin requirement for most animals[3] and that quinolinate is known to modify the activities of several important enzymes and biological processes.[4] Our interest in quinolinic acid biosynthesis arose from the observation that purified preparations

(1) (a) This work was supported by a research Grant (AM 13448) from the National Institute of Arthritis, Diabetes, and Digestive and Kidney Diseases, Public Health Service. (b) Taken from the Ph.D. Thesis of L.D.K., The Pennsylvania State University, 1983.

(2) Nishizuka, Y.; Ichiyama, A.; Hayaishi, O. *Methods Enzymol.* **1970**, *17A*, 463-466.

(3) Krehl, W. A.; Tepley, L. J.; Sarma, P. S.; Elvehjem, C. A. *Science (Washington, DC)* **1945**, *101*, 489-490. Henderson, L. M.; Ramasarma, G. B.; Johnson, B. C. *J. Biol. Chem.* **1949**, *181*, 731-738. Hundley, J. M. *Vitamins* **1954**, *2*, 578.

(4) Veneziale, C. M.; Walter, P.; Kneer, N.; Lardy, H. A. *Biochemistry* **1967**, *6*, 2129-2138. MacDonald, M. J. *Biochem. Biophys. Res. Commun.* **1979**, *90*, 741-749. Hsu, S. L.; Fahein, L. A. *Arch. Biochem. Biophys.* **1976**, *177*, 217-225. Various authors *Am. J. Clin. Nutr.* **1971**, *24*, 651-851.

0002-7863/87/1509-2156$01.50/0

Scheme I

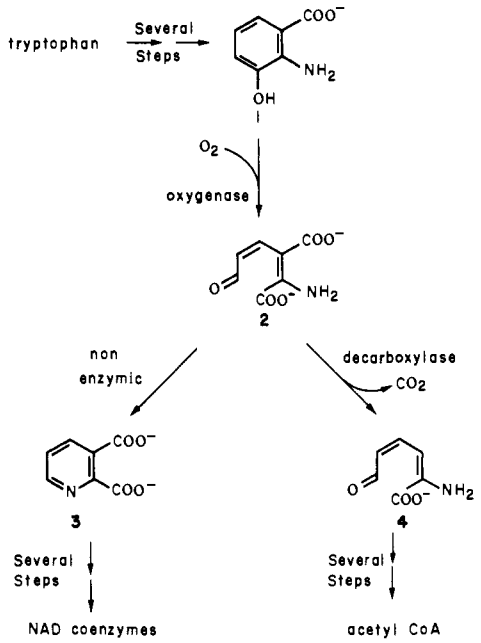

of *myo*-inositol oxygenase are activated by quinolinate under certain conditions.[5]

One curious feature of quinolinic acid biosynthesis in animals is that the conversion of α-amino-β-carboxymuconate ε-semialdehyde (**2**) to quinolinate (**3**), and thus ultimately to the nicotinamide coenzymes, is widely believed to occur physiologically by a nonenzymic reaction that is competing with an enzymic reaction at a branchpoint in the pathway. Such a situation is certainly unusual in biological systems if not unique; the authors are aware of no other related examples. Since the literature does not contain detailed descriptions of the attempts of others to identify an enzyme for the cyclization to quinolinate, we have searched for such an enzyme,[1b] and, like others, have failed to detect any evidence that an enzyme for this step is present. Because of the significance of the pathway and thus of this nonenzymic step in animal metabolism it seemed important to clarify the mechanistic details of the reaction and to determine what small molecules might affect its rate in vivo. Such a study is reported here.

The mechanistic questions which have to be addressed in the cyclization of **2** to **3** are outlined in Scheme II. It is expected that the immediate product of the oxygenase reaction is the *Z* isomer **2**, but in order to cyclize, isomerization to the *E* isomer **6** must occur. This could occur by an uncatalyzed thermal isomerization, a pericyclic mechanism through **5**, or by some catalyzed process, possibly by formation of an addition intermediate. For example, enzymes which catalyze other cis–trans isomerizations are known to proceed through a thiol addition intermediate.[6] The ring closure step forming the carbinolamine **9** from **6** might proceed by an intramolecular carbonyl addition reaction either with or without formation of zwitterionic addition intermediate **7** with a kinetically significant lifetime or alternately through a pericyclic reaction involving **8**, formed from **6**. Loss of water from **9** then results in formation of the aromatic Schiff base, namely quinolinate.

It has been found in this work that the isomerization step is kinetically insignificant in the conversion of **2** to **3**. Furthermore, through a detailed examination of the effects of pH, buffers, D_2O, and deuterium labeling of **2** on the kinetics of this reaction, it appears that either carbinolamine formation or dehydration can be rate determining depending on experimental conditions.

(5) Reddy, C. C.; Pierzschala, P. A.; Hamilton, G. A. *J. Biol. Chem.* **1981**, *256*, 8519–8524. Reddy, C. C.; Hamilton, G. A. *Biochem. Biophys. Res. Commun.* **1981**, *100*, 1389–1395.

(6) Seltzer, S. *The Enzymes* **1972**, *6*, 381–406.

Scheme II

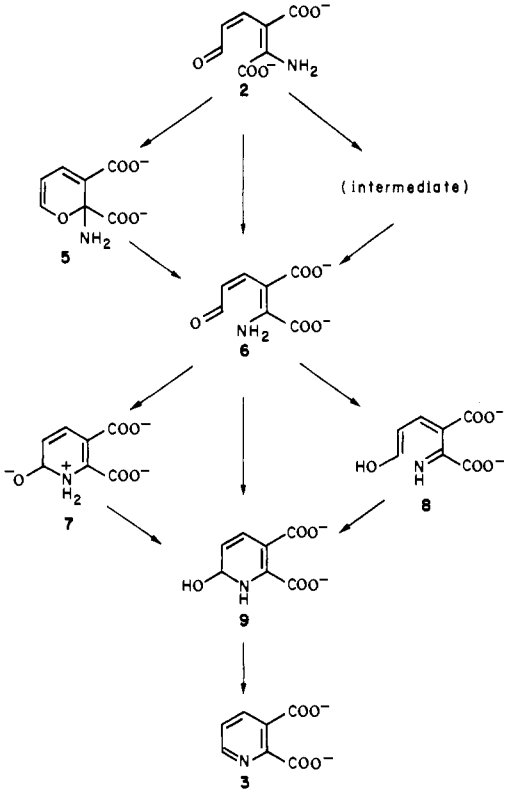

Experimental Section

General Methods. All melting points are reported uncorrected. Routine UV–vis absorption spectra were recorded on a Hitachi Model 100-80 or a Cary 118 spectrophotometer. Kinetic results were obtained on a Gilford Model 240 spectrophotometer equipped with an automatic sampler changer, strip chart recorder, and constant temperature bath. Proton nuclear magnetic resonance (^{1}H NMR) spectra were measured with a Varian EM 360 spectrometer by using tetramethylsilane as an internal standard ($\delta = 0$) in Me_2SO-d_6. Mass spectral data were obtained by using a Finnegan 3200 gas chromatograph/mass spectrometer equipped with a Finnegan 6000 data system.

Materials. Unless otherwise noted, reagent grade or better commercial materials, obtained from Sigma Chemical Co. or Fisher Scientific Co., were dried in vacuo and used without further purification. Imidazole and hydroxylamine hydrochloride were recrystallized from benzene and ethanol, respectively, and dried in vacuo. Ethylamine, ethanolamine, and triethylamine were distilled prior to use; these and other bases employed were >99% pure (by titration). Buffer solutions were prepared by dissolution of either weighed amounts of the acid and base forms of the buffer material and KCl or weighed amounts of base and KCl, plus an appropriate volume of standard HCl solution, followed by dilution in volumetric flasks. Small pH adjustments (always less than 0.05 pH unit) were made, when necessary, by using concentrated HCl or 50% KOH. Solutions of pH less than 2 and greater than 12 were prepared by using dilutions of standard HCl or KOH, respectively, containing appropriate KCl to maintain ionic strength. The pH values of these solutions were calculated based on the titratable concentrations of H^+ or OH^-. Solvent isotope effect studies employed D_2O (99.8% atom D, Sigma) as solvent. Adjustments of pD were made by using 35% DCl in D_2O (>99% atom D, Sigma) or concentrated NaOD prepared by dissolution of sodium metal in D_2O. Acetate buffers in D_2O were prepared by using CD_3CO-OD (99.5% atom D, Sigma) and CD_3COONa (>99% atom, D, Sigma). Tris buffers in D_2O were prepared by using deuterated Tris, obtained by thrice recrystallizing Tris base from D_2O, and deuteriated Tris deuteriochloride, obtained by acidifying concentrated deuteriated Tris solution with DCl, then crystallizing, collecting, and drying the products in vacuo. All H_2O used in this research was either (a) doubly distilled, the second time with a Kontes WS-2 glass still following passage through Barnstead organic and ion exchange columns or (b) glass distilled and then passed through a Millipore reverse osmosis water purification system.

3-Hydroxyanthranilate Oxygenase. Partially purified enzyme was prepared following a published procedure[7] through and including step 2 (ammonium sulfate fractionation). A typical preparation had a specific activity of 24 mkat/kg (1 kat equals 1 mol per s) when measured at 25 °C, pH 6.5, with 0.20 mM 3-hydroxyanthranilate (**1**) and 50 mM KCl

present. The protein was not homogenous, but it had insignificant decarboxylase activity when **2** is used as a substrate. This enzyme solution could be stored indefinitely (>1 year) at −20 °C without appreciable loss of activity.

α-Amino-β-carboxymuconic ε-Semialdehyde (2). In a typical case 3.7 mg (1.2 μmol) of reduced glutathione and 2.3 mg (0.8 μmol) of $Fe(NH_4)_2(SO_4)_2$ (both dissolved in H_2O) were added to 15 mg of the 3-hydroxyanthranilate oxygenase preparation at room temperature in a final volume of 5.8 mL (the pH was 3.5–4.5 at this point). After incubating for 3 min to activate the enzyme,[7] 18.2 mL of H_2O was added, and the solution was carefully adjusted to pH 7.3, by using dilute aqueous KOH. The resulting solution was rapidly stirred for 15 min with periodic adjustment to pH 7.3. The reaction was initiated by adding 1.47 mg (9.6 μmol) of 3-hydroxyanthranilic acid dissolved in H_2O and adjusted to pH 7.4. The progress of the oxidation was monitored by following the appearance of **2** as indicated by the absorbance at 360 nm of 30 μL aliquots of the reaction mixture diluted to 3.00 mL with pH 7.40, 50 mM Tris chloride buffer. When the absorbance had reached a maximum (2–4 min), the reaction mixture was transferred to a cooled (ice–water bath) container, mixed with an equal volume of ice cold $CHCl_3$ (to inactivate and precipitate the protein), then vigorously shaken, and briefly centrifuged (all further operations were carried out at 0–4 °C). The nearly transparent aqueous layer was withdrawn and immediately frozen in liquid N_2. Solutions of **2** prepared in this manner were stable for several months at −70 °C. In later kinetic experiments, some **2** preparations were concentrated by partial lyophilization, providing solutions which were kinetically and spectrophotometrically indistinguishable from samples which had not been concentrated by using this method.

Deuterium-Labeled 3-Hydroxyanthranilic Acid (1-d_1 and 1-d_2). 3-Hydroxyanthranilic acid (0.77 g, 5.0 mmol) and 10 mL of D_2O were mixed, and a concentrated NaOD solution was added dropwise until all the solid had dissolved. The pD was adjusted to pD 11.1 (pH meter reading +0.4),[8] and the solution was sealed in a glass tube. For the preparation of **1-d_1** the solution was heated for 69 h at 74 °C whereas for **1-d_2** the solution was heated at 82 °C for 145 h, then transferred to a suitable container, and refluxed for 48 h. Periodically aliquots of this solution were removed and cooled to room temperature, and the ^1H NMR spectra recorded. When exchange had occurred to the desired extent, the dark brown solution was cooled to room temperature, and the pH was adjusted by using concentrated HCl to pH 3.85 (measured by the pH meter), with precipitate appearing at pH 6–6.5. After having been cooled to 0 °C, the resulting solid was collected, washed with 10 mL of H_2O, and dried in vacuo. This material was twice recrystallized following a published procedure.[9] Yield of **1-d_2**: 0.154 g (20%) of pale tan crystals, mp 257 °C (d).

Deuterium-Labeled α-Amino-β-carboxymuconic ε-Semialdehyde. This was prepared by using deuterium-labeled 3-hydroxyanthranilic acid and the standard enzymic procedure given above. The identity of the product was confirmed by its UV–vis spectrum and its characteristic pH dependent spectral changes.[10] The presence of deuterium at the aldehydic carbon is indicated by (a) a significant kinetic secondary isotope effect in its conversion to quinolinic acid and (b) the kinetic secondary isotope effect was the same for **2-d_1** and **2-d_2** (see Results section for the actual deuterium content of these materials).

Kinetics. Kinetic runs were initiated by the addition of 0.03 mL of a stock solution of **2** to 3.00 mL of the desired buffer solution which had been temperature equilibrated (>20 min) and stoppered. The final concentration of **2** was less than 4 μM. The progress of the reaction was followed by observing the change in optical density at 360 nm (in neutral and basic solution, ϵ = 47 500) above pH 5 and at 345 nm (ϵ ca. 35 000) below pH 5 through 5–10 half-times. All reactions displayed pseudo-first-order kinetics to >3 half-times and k_{obsd} was taken as the negative slope from a plot of ln (OD_t − OD) vs. time. In some cases, a small correction was made[1b] based on the small linear drift in the base line observed after completion of the reaction. The temperature and pH of buffer solutions was checked before and after each run. Solvent isotope effects were studied by simultaneously following the reaction of **2** in H_2O and D_2O buffer solutions at the same buffer ratios and concentrations. Kinetic secondary deuterium isotope effect experiments were run in parallel, by using labeled and unlabeled **2**. The effect of light was ascertained by measuring the $OD_{360\ nm}$ at various time intervals of aliquots of simultaneously equilibrating solutions of **2** (pH 7.5, 20 mM phosphate buffer, 0.05 M ionic strength, maintained with KCl, 37 °C), one flask wrapped in black electrical tape, and the other 30 cm from a 275-W Sunlamp (flask was 50 mL, Pyrex, no. 4980; light passing through glass into the solution). The lack of an effect of O_2 on the reaction was determined by purging a buffered solution with O_2 (>15 min) or N_2 (>1 h) prior to use. Thereafter, no special precautions were taken to exclude oxygen from buffer solutions except in the survey of possible catalysts; in cases where a particularly readily oxidizable compound was being employed, O_2 was again excluded.

Determination of a pK_a of 2. The UV–vis spectrum of **2** undergoes significant reversible changes in the pH 4–7 range, allowing determination of the pK_a of one of the acid groups of **2** according to a general method given by Albert and Serjeant.[11] The pK_a was calculated from the data by using eq 1, where A_m, A_i, and A are the respective zero time absorbances of the fully unprotonated, fully protonated, and partially protonated **2** at that particular pH.

$$pK_a = pH + \log (A - A_m)/A_i - A) \quad (1)$$

Reaction Products Formed from 2 at Various pH Values. Aliquots (44 μL) of a stock solution of **2** were quickly added to each of 4.50 mL of 20 mM buffers (same as spectrophotometric titration buffers) which had been equilibrated to 37 °C. After reaction was complete (>10 half-times for the slowest reactions), the solutions were each made basic to greater than pH 11 by addition of 3 drops of 50% KOH, and the spectra were recorded at room temperature between 400 and 240 nm.

Results

General Characteristics of the Reaction of 2. Previous investigations[9,12] had indicated that, near neutral pH, **2** reacts to give essentially a quantitative yield of quinolinic acid, and this was confirmed in the present research. At all pH values above 4.5, quinolinic acid is the only product that can be detected by thin-layer chromatography, and the increase in absorbance at 265 nm corresponds exactly to the decrease at 360 nm when the extinction coefficients of quinolinic acid (ϵ = 3400 M^{-1} at 268 nm) and **2** (ϵ = 47 500 M^{-1} at 360 nm) are taken into account. As others have noted,[9,12] **2** is converted in acid solution to another product, namely α-hydroxymuconic ε-semialdehyde. In the present research, it was found that this product can be detected spectrophotometrically only when the reaction of **2** proceeds below pH 4. Because this semialdehyde only appears at pH values far removed from the physiological pH, an extensive investigation of the relative yields of quinolinic acid and α-hydroxymuconic ε-semialdehyde as a function of pH was not undertaken.

Under all conditions examined in the present research, **2** reacts according to first-order kinetics; such plots of the data are linear for at least 2 to 3 half-times. In preliminary experiments, it was established that the presence or absence of either light or O_2 has no effect on the observed first-order rate constant. However, it was found that the rate constant does depend on the ionic strength, pH, and buffer concentration, so when studying the effect of one of these variables the others were strictly controlled.

Survey of Potential Catalysts. Since **2** contains a number of functional groups, it seemed possible that its conversion to quinolinate might be catalyzed by various small molecules (some of which could be present physiologically). However, at 37 °C, in 50 mM tris·HCl buffer, pH 7.40, μ = 0.50 M (KCl), the following compounds at 10 mM concentrations (except where indicated) affect the rate of the conversion by less than 35%; (a) carbonyl compounds (which could have formed a Schiff base with the amino group), such as formaldehyde, acetaldehyde, glyoxylate, and pyridoxal 5′-phosphate (1.0 mM); (b) nucleophiles (which might have added to the conjugated double bond system to increase the rate of a cis-trans isomerization), such as glutathione, ethanethiol, (D,L)-cysteine, β-mercaptoethylamine, ethylamine, benzylamine, and hydroxylamine; (c) metal ions (all at 1.0 mM concentration) such as $MgCl_2$, $CuCl_2$, $ZnCl_2$, $CaCl_2$, $CoCl_2$, $NiCl_2$, $Fe(NH_4)_2SO_4)_2$, and $Mn(acetate)_2$; and (d) cofactors (all at 1.0 mM except where indicated) such as coenzyme A, NAD^+,

(7) Koontz, W. A.; Shiman, R. *J. Biol. Chem.* **1976**, *251*, 368–377.
(8) Fife, T. H.; Bruice, T. C. *J. Phys. Chem.* **1961**, *65*, 1079–1080.
(9) Miyake, A.; Bokman, A. H.; Schweigert, B. S. *J. Biol. Chem.* **1954**, *211*, 391–403.
(10) Ichiyama, A.; Nakamura, S.; Kawai, H.; Honjo, T.; Nishizuka, Y.; Hayaishi, O.; Senoh, S. *J. Biol. Chem.* **1965**, *240*, 740–749.
(11) Albert, A.; Serjeant, E. P. *The Determination of Ionization Constants*; Chapman and Hall: London, 1971; Chapter 4.
(12) Long, C. L.; Hill, H. N.; Weinstock, I. M.; Henderson, L. M. *J. Biol. Chem.* **1954**, *211*, 405–417. Wiss, O.; Simmer, H.; Peters, H. *Hoppe-Seyler's Z. Physiol. Chem.* **1956**, *304*, 221–231. Kuss, E. *Hoppe-Seyler's Z. Physiol. Chem.* **1967**, *348*, 1602–1608. Mehler, A. H. *J. Biol. Chem.* **1956**, *218*, 241–254.

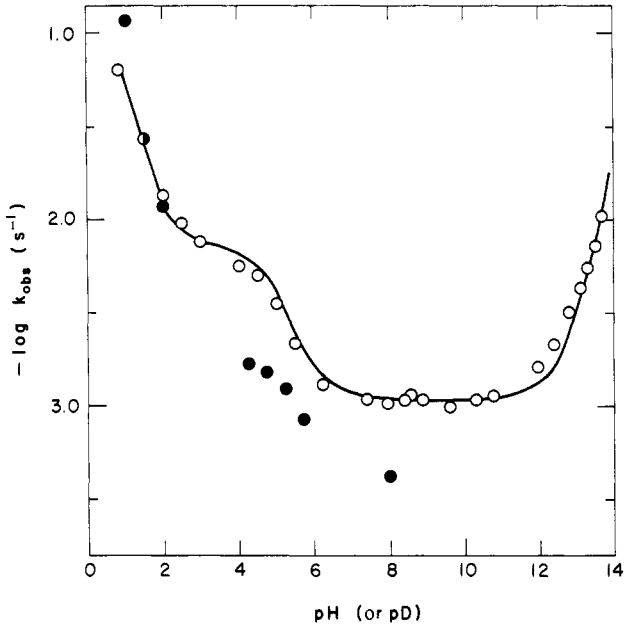

Figure 1. The effect of pH (and pD[8]) on the observed first-order rate constant for the disappearance of **2** in H_2O (○) and D_2O (●). Reaction conditions: 37 °C, μ = 0.50 M (KCl). The data have been extrapolated to zero buffer concentration where appropriate. Below pH 2 and above pH 11 the data were obtained by using HCl and KOH solutions, respectively. The curve through the H_2O data was calculated by using the constants and kinetic scheme described in the text.

NADH, $NADP^+$, NADPH, FAD (0.1 mM), ATP, UTP, and cyclic AMP (10 mM).

Effects of pH. As illustrated by the results shown in Figure 1, the first-order rate constant (extrapolated to zero buffer concentration) for the reaction of **2** is pH dependent below pH 7 but is independent of pH from approximately 7–11. The shape of the curve indicates that there is an acid-catalyzed reaction at low pH, and at an intermediate pH (from 3 to 6) some protonated species reacts more rapidly than the species present at pH's above 7. Because **2** undergoes reversible spectral changes in the pH 4–6 region, it is possible to obtain a pK_a for this protonated species. A value of about 5.0, which is largely independent of ionic strength (0.05–0.15 M) and temperature (from 20 to 37 °C), was found. As indicated earlier, quinolinic acid is the only product at pH values above 4.5 so that part of the curve corresponds exclusively to its formation from **2**. The acid-catalyzed reaction that becomes significant below pH 3 is due to the reaction forming α-hydroxymuconic semialdehyde.

The pH dependence of the reaction in H_2O can be rationalized in terms of the kinetic mechanism shown in eq 2 where proton

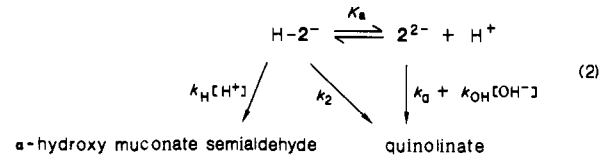

(2)

and hydroxide catalysis are represented by k_H and k_{OH} respectively; k_2 is the plateau rate near pH 4, and k_0 corresponds to the pH independent reaction between pH 7 and 11. The rate law corresponding to the mechanism of eq 2 is given in eq 3. The curve in Figure 1 was calculated by using this equation and the following constants: $k_H = 0.54\ M^{-1}\ s^{-1}$, $k_2 = 7.0 \times 10^{-3}\ s^{-1}$, $k_0 = 1.10 \times 10^{-3}\ s^{-1}$, $k_{OH} = 1.85 \times 10^{-2}\ M^{-1}\ s^{-1}$, $K_a = 1.0 \times 10^{-5}$ M and $K_W = 1.0 \times 10^{-14}$.

$$k_{obsd} = \frac{(k_H[H^+] + k_2)[H^+] + (k_0 + k_{OH}K_W/[H^+])K_a}{[H^+] + K_a} \quad (3)$$

Effects of Buffer. In the plateau region at pH 4.5 there is very little effect of buffer concentration on the reaction rate. For example, increasing the sodium acetate–acetic acid concentration from 20 to 500 mM (37 °C, 0.5 M ionic strength) increases the rate of disappearance of **2** by less than 15%, and the small increase that is observed appears to depend linearly on the buffer concentration. In contrast, at pH values of 7–11, where the reaction velocity is independent of pH, there is a marked dependence of the rate on the nature and concentration of buffer. For example, using Tris as the buffer, the results shown in Figure 2 are obtained. Thus, at low concentrations the rate increases with buffer concentration, but a maximum rate is reached at higher concentrations. It was shown[1b] that this increase is not due to some general or specific salt effect; the same effect of Tris concentration on the rate is observed when the total ionic strength is varied from 0.05 to 3.0 M or if the KCl usually used to maintain ionic strength is replaced by KNO_3 or NaCl. Furthermore, effects very similar to those illustrated in Figure 2 are observed when Tris is replaced by several other buffer species. Some are more effective at increasing the rate of the reaction than others at low concentrations, but in each case the observed first-order rate constant increases with buffer concentration at low concentrations but reaches a maximum at higher concentrations. In some cases, the rate decreases at even higher buffer concentrations, but that is probably due to a medium effect. The total increase in rate caused by buffers varies from about 50 to 150% depending on temperature (the larger effects are seen at higher temperatures).

A similar nonlinear buffer dependence has been seen in other carbonyl group reactions[13] and has been interpreted as indicating

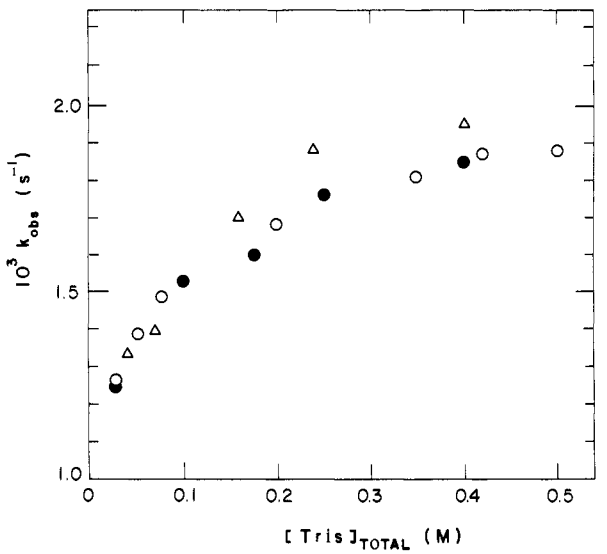

Figure 2. The effect of Tris buffer concentration on the observed first-order rate constant for the reaction of **2** at pH 7.40 (○), 7.99 (△), and 8.56 (●). Reaction conditions: 37 °C, μ = 0.50 M (KCl).

Table I. Catalytic Constants for Catalysis by Buffers of One Step in the Conversion of **2** to **3**[a]

catalyst	pK_a	10^2k M^{-1} s^{-1}	10^2k M^{-1} s^{-1}
phosphate	6.79	<9.2[b]	<2.3[b]
imidazole	6.96	4.3	4.9
triethanolamine	7.98	<4.1[b]	<4.1[b]
Tris	7.99	3.8	2.5
triethylenediamine	8.87	3.3	1.6
carbonate	9.74	0.62	1.9
triethylamine	10.79	<0.3[b]	<0.1[b]
H_2O	15.74	0.004	

[a] Data collected at 37 °C, μ = 0.50 M (KCl). [b] Since these were studied at only one pH or over a limited pH range, only upper limits can be assigned to these constants.

(13) Cordes, E. H.; Jencks, W. P. *J. Am. Chem. Soc.* **1962**, *84*, 4319–4328. Eriksson, S. O.; Holst, C. *Acta Chem. Scand.* **1966**, *20*, 1892–1906. Eriksson, S. O.; Bratt, L. *Acta Chem. Scand.* **1967**, *89*, 917–922. Cunningham, B. A.; Schmir, G. L. *J. Am. Chem. Soc.* **1967**, *89*, 917–922. Sayer, J. M.; Jencks, W. P. *J. Am. Chem. Soc.* **1969**, *91*, 6353–6351. Sayer, J. M.; Jencks, W. P. *J. Am. Chem. Soc.* **1973**, *95*, 5637–5649.

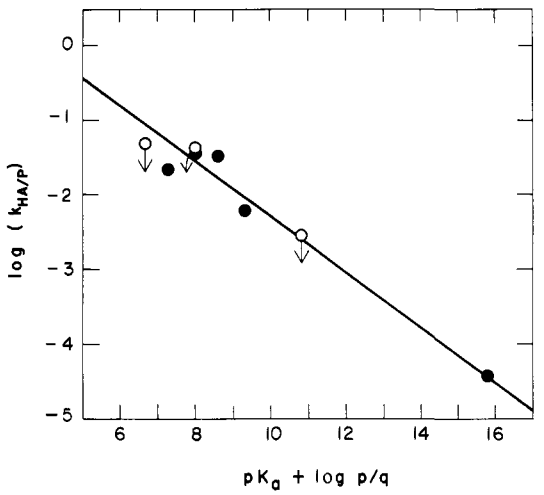

Figure 3. A Brønsted plot for catalysis of **2** cyclization by buffer acids in the pH range 6.5–11, 37 °C, μ = 0.50 M (KCl): (●) from left to right, imidazolium, Tris H^+, triethylene diamine H^+, bicarbonate, and H_2O; (♀) from left to right, upper limits for catalysis $H_2PO_4^-$, triethanolamine H^+ and triethylamine H^+.

a change in the rate-determining step in a stepwise mechanism. Thus, the present results are considered strong evidence that the reaction proceeds in a minimum of two steps with at least one kinetically important intermediate.

An examination of the data obtained by using various buffers at different pH values reveals significant catalysis by both the acidic and basic forms of the buffer. When the data are corrected for a change in the rate-determining step,[1b,14] catalytic constants for the various buffer species are obtained, and these are given in Table I. A Brønsted plot for catalysis by general acids is shown in Figure 3 from which an α of 0.3–0.4 is indicated even if the data point for water is excluded. For catalysis by general bases, generally smaller catalytic constants are seen, and a satisfactory Brønsted plot was not obtained.[15]

D_2O Effects. As indicated in Figure 1, above pH 4 the reaction forming quinolinate (extrapolated to zero buffer concentration) proceeds with a normal solvent deuterium isotope effect. Below pH 4 the solvent isotope effect decreases and becomes inverse below ca. pH 1.5 as expected for the acid-catalyzed reaction forming α-hydroxymuconate semialdehyde.

When the dependence of the reaction velocity on Tris buffer concentration is compared in D_2O and H_2O, it is found that a large change in solvent isotope effect occurs, and this parallels the observed change in the rate-determining step. The results in Figure 4 demonstrate that the sovlent isotope effect of ≥2.3 at low buffer concentration decreases to a limiting value of ≤1.1 at high buffer concentration. When these data are corrected for a change in rate-determining step,[1b,14] the plots shown in Figure 5 are obtained. From the intercepts, one then can calculate that at zero buffer concentration the solvent deuterium isotope effect, k_{H_2O}/k_{D_2O}, is 3.9. From the slopes, the isotope effect on the Tris buffer-catalyzed reaction is calculated to be 1.5. This is the net isotope effect for catalysis by both the acid and base forms of Tris, but since >80% of the catalysis under the conditions of these experiments is due to the acid form, the value of 1.5 probably largely reflects the ratio

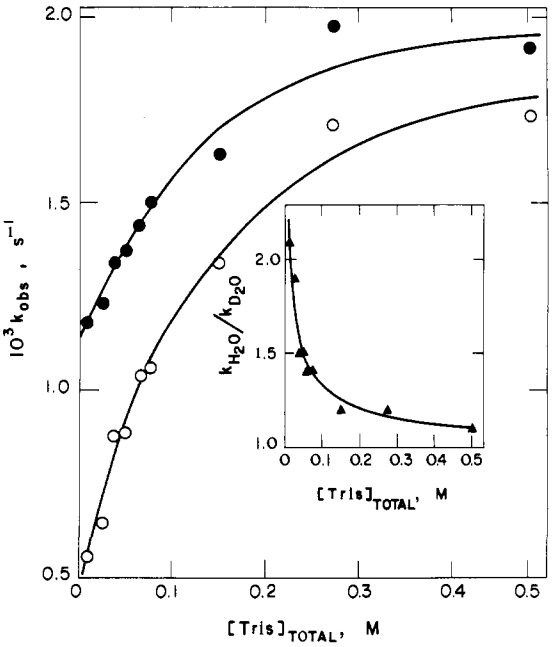

Figure 4. The effect of Tris buffer concentration on the observed first-order rate constant for **2** disappearance in H_2O (●) and D_2O (○). Reaction conditions: 37 °C, μ = 0.50 M (KCl), buffer ratio (HA/A) = 3.16. The insert is a replot of the data emphasizing the dependence of the solvent isotope effect (k_{H_2O}/k_{D_2O}) on the Tris buffer concentration.

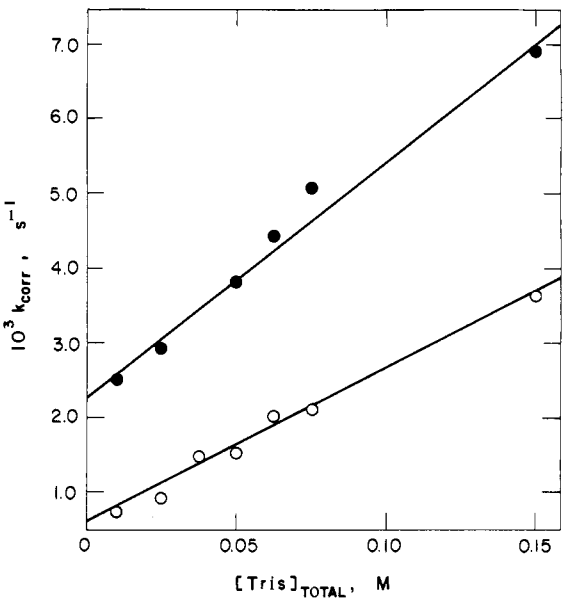

Figure 5. The effect of Tris buffer concentration on the corrected first-order rate constant for **2** disappearance in H_2O (●) and D_2O (○). Reaction conditions: same as in Figure 4. $k_{corr} = k_{obsd}/(1 - k_{obsd}/k_\infty)$ where k_∞ is the value of the rate constant at infinite catalyst concentration.

k_{HTris}/k_{DTris}. In any event, the observation of an isotope effect for both the water- and buffer-catalyzed reactions suggests that proton transfers are occurring in the rate-determining steps for both. This result is consistent with the observation of apparent Brønsted catalysis by buffer acids.

Secondary Deuterium Isotope Effect. In order to examine the effect of deuterium substitution at the aldehydic carbon of **2**, the aromatic protons of **1** were exchanged by prolonged heating in alkaline D_2O. The exchange reaction is readily followed by ^1H NMR with the relative rates of aromatic proton exchange being o > p >> m (positions relative to the OH group) as expected. Proton NMR and mass spectral analysis of the exchanged **1** isolated from acidified solutions clearly shows the presence and position of deuterium in the aromatic ring.[1b] Two labeled samples

(14) Hogg, J. L.; Jencks, D. A.; Jencks, W. P. *J. Am. Chem. Soc.* **1977**, *99*, 4772–4778.

(15) Basic primary amine buffers, such as ethanolamine and ethylamine, react differently with **2** (at pH values above 9) than any of the species listed in Table I.[1b] With the basic primary amines, it is evident that the amine reacts with **2** to give a Schiff base (λ_{max} ~ 395 nm) which then only slowly disappears, at a rate that is about an order of magnitude slower than the uncatalyzed **2** to **3** conversion itself. Thus, rather than catalyzing this conversion, the basic primary amines actually slow it down. There is some evidence that hydroxylamine catalysis may occur partially by this mechanism as well,[1b] but there is no evidence that Tris (the one buffer in Table I that could conceivably function by this mechanism) reacts by such a mechanism. Since the reaction does not occur at neutral pH with the types of amines likely to be encountered physiologically, it has not been extensively investigated.

Table II. Kinetic Secondary Deuterium Isotope Effects for the Conversion of **2** to Quinolinate at Various Buffer Concentrations[a]

[Tris], mM	$10^3 k^{H}_{obsd}$, [b,c] s^{-1}	$10^3 k^{D}_{obsd}$, [b,d] s^{-1}	k^{D}_{obsd} [e]$/k^{H}_{obsd}$
25	1.29	1.43	1.15
50	1.41	1.57	1.16
150	1.66	1.80	1.12
270	1.89	2.06	1.12
500	1.84	1.99	1.11

[a] Reaction conditions: 37 °C, pH 7.40, μ = 0.50 M (KCl). [b] Each number is the average of four independent determinations, and the data for **2-*d*$_1$** were obtained simultaneously with the data for unlabeled **2**. Thus, for each concentration of Tris, two sets of experiments were run; the curvette carriage, which contained four curvettes, had in each set of experiments two curvettes containing **2-*d*$_1$** and the other two containing unlabeled **2**. [c] Obtained by using unlabeled **2**. [d] Obtained by using **2-*d*$_1$**. [e] Corrected for the fact that **2-d$_1$** has only 73% deuterium in the aldehydic position. In other experiments in which the reactant was **2-*d*$_2$** essentially indentical ratios were obtained.

were prepared, **1-*d*$_1$**, which has on average approximately one deuterium per molecule and has specifically 73% of its molecules labeled with deuterium in the ortho position, and **1-*d*$_2$** which has on average approximately two deuteriums per molecule with the ortho position being essentially 100% labeled and the rest mainly in the para position. Enzyme-catalyzed oxidation of labeled **1** is expected to yield **2** with the same degree of deuterium labeling, i.e., the aldehyde carbon of **2** should have the same amount of deuterium as the ortho position of **1**.

By using either **2-*d*$_1$** (prepared from **1-*d*$_1$**) or **2-*d*$_2$** (prepared from **2-*d*$_2$**), the same kinetic secondary deuterium isotope effect is obtained, after correcting for the less than 100% deuterium content at the aldehydric carbon of **2-*d*$_1$**. As indicated in Table II, the secondary isotope effect does not vary (within experimenal error) throughout the change in the rate-determining step seen by using Tris buffers at pH 7.4. The average effect obtained by using this range of Tris buffer concentrations is k_D/k_H = 1.14. The results indicate that, in going from reactant to either transition state (at low or high buffer concentration), there is a net change of sp^2 to partial sp^3 hybridization occurring at the aldehyde carbon.[16,17]

Discussion

Since the major focus of this study is the elucidation of the mechanism of quinolinate formation under physiological conditions, the discussion will be concerned mainly with the reaction of **2** observed in the pH independent region from pH 7 to 11. Reactions occurring in other pH ranges will be briefly considered at the end of the discussion.

The results clearly indicate that geometric isomerization is never rate limiting in the conversion of **2** to quinolinate. The result that most convincingly supports this conclusion is the inverse kinetic secondary deuterium isotope effect seen under all conditions examined. Such an effect is not consistent with the uncatalyzed modes of isomerization depicted in Scheme II.[16] Further, though not conclusive, support for rapid isomerization is the observation that compounds such as thiols do not significantly alter the rate of the reaction.[6] The mechanism for the isomerization of **2** to **6** is not known. The rapid isomerization may simply occur because of the considerable single bond character in the bond undergoing rotation in this vinylogous amide (others[18] have observed that vinylogous amides and related compounds isomerize rapidly under mild conditions), or it may possibly occur with a conformer of **8** and **8** as intermediates. In any event, the results indicate that these species are probably in rapid equilibrium; in fact, the stock solution of the reactant is very likely an equilibrated mixture of the two.

The above conclusion compels one to consider that a step associated with either cyclization (**6** to **9**, Scheme II) or loss of water (**9** to **3**) is rate determining under any given set of conditions. As indicated in the Results section, the evidence is quite clear that there is a change in the rate-determining step as the buffer concentration is increased. Thus, the question comes down to deciding which of the steps in the **6** to **9** to **3** conversion is rate determining at low buffer concentrations and which at high buffer concentrations. As an aid to making this decision, it is useful to summarize the observed characteristics of the reaction under these two sets of conditions. At low buffer concentrations the reaction (a) is catalyzed by general acids and, less effectively, by general bases, (b) proceeds more slowly in D_2O than in H_2O (measurable solvent isotope effects are observed for both the uncatalyzed and buffer-catalyzed parts), and (c) proceeds with a significant inverse kinetic secondary deuterium isotope effect. On the other hand, at high buffer concentrations the reaction (a) is not catalyzed by acids or bases, (b) proceeds at essentially the same rate in D_2O as in H_2O, but (c) also proceeds with a significant inverse kinetic secondary deuterium isotope effect.

Parts (a) and (b) of the above summaries strongly imply that at low buffer concentration the rate-determining step involves a proton transfer while at high buffer concentration a proton transfer does not occur in the rate-determining step. Considering the possible steps in the **6** to **3** conversion, Scheme II, the only one that could reasonably be expected to proceed without proton transfers would be either the **6** to **7** step or the **8** to **9** pericyclic reaction. Such considerations indicate, therefore, that the direct conversion of **6** to **9** (without an intermediate) cannot be occurring because both it and the subsequent dehydration step to give **3** both require proton transfers. Consequently, the steps involving proton transfers that need to be considered as possibly rate determining at low buffer concentrations are the **6** to **8**, **7** to **9**, and **9** to **3** steps.

Of these latter steps, the possibility that **7** to **9** is ever rate determining can be eliminated for the following reasons. First, the observed value for the secondary deuterium isotope effect (k_D/k_H = 1.14) is considerably smaller than that observed for a complete sp^2 to sp^3 hybridization change. As examples, K_D/K_H = 1.36 for hydroxylamine addition to benzaldehyde and 1.37 for hydration of acetaldehyde.[19,20] Since the transition state for the **7** to **9** conversion has a completely formed sp^3 carbon, one would thus expect a higher secondary deuterium effect if this were the rate-determining step at low buffer. A second argument against this step being the important buffer-catalyzed step is that bifunctional catalysts, such as phosphate monoanion and bicarbonate, do not show any catalytic advantage compared to monofunctional acids and bases, whereas they frequently do in other cases where this mechanism is operative.[21] Finally, although the buffer catalysis data are limited, at least for buffer acids, the Brønsted plot (Figure 3) appears linear, with a significant Brønsted coefficient (α = 0.3–0.4), and there is no indication of the Eigen type behavior required for such a trapping mechanism.[22]

(16) Shiner, V. J., Jr. In *Isotope Effects in Chemical Reactions*; Collins, C. J., Bowman, N. S., Eds.; Van Nostrand: New York, 1970; pp 90–159.

(17) The kinetic secondary deuterium isotope effect was also measured at pH 4.75 (50 mM potassium acetate buffer, 37 °C, μ = 0.50 M) and found to be k_D/k_H = 1.11 ± 0.05.

(18) Prokofbev, E. P.; Krasnaya, Z. A.; Kucherov, B. F. *Isv. Akad. Nauk S.S.S.R., Ser. Khim.* **1973**, *9*, 2013–2022. Shvo, Y.; Taylor, E. C.; Bartulin, J. *Tetrahedron Lett.* **1967**, *34*, 3259–3265. Shvo, Y.; Shanan-Atidi, H. *J. Am. Chem. Soc.* **1969**, *91*, 6683–6688; 6689–6696. Marvell, E. N.; Caple, G.; Gosink, T. A.; Zimmer, G. *J. Am. Chem. Soc.* **1966**, *88*, 619–620.

(19) do Amaral, L.; Bastos, M. P.; Bull, H. G.; Cordes, E. H. *J. Am. Chem. Soc.* **1973**, *95*, 7369–7374. Lewis, C. A., Jr.; Wolfenden, R. V. *Biochemistry* **1977**, *16*, 4886–4890.

(20) A reviewer has suggested that possibly the reason the kinetic secondary deuterium isotope effect is less than the maximum for a complete sp^2 to sp^3 conversion is because the carbonyl group of the reactant is partially hydrated (it would need to be about 60% hydrated to explain the results assuming the transition state has complete sp^3 hydridization). This seems very unlikely for several reasons, including the following: (a) the UV absorption at 360 nm with its high extinction coefficient (47 500 M^{-1} cm^{-1}) is not consistent with a major part of the reactant being the hydrate, (b) the complexing of metal ions might be expected to alter any hydration–dehydration equilibrium, and yet metal ions have no significant effect on the absorption at 360 nm, and (c) one would not expect the carbonyl group of vinylogous amides to be hydrated because that would lead to complete loss of the amide resonance (the sluggishness with which **2** reacts with carbonyl group reagents[12] is an indication that the vinylogous amide resonance is considerable).

(21) Cox, M. M.; Jencks, W. P. *J. Am. Chem. Soc.* **1981**, *103*, 580–587.

The possibility that the **6** to **8** conversion could be the rate-limiting step at low buffer can also be eliminated because there is no change in hybridization at the original aldehyde carbon in this transformation, and thus no kinetic secondary deuterium isotope effect would be expected. This step is expected to be rapid in any event since it involves proton transfers to and from oxygen and nitrogen centers. Although rate-determining proton transfers to and from such centers resident on unstable intermediates have been observed, that would not be expected to occur with a relatively stable compound such as **6**.

As a result of the above considerations, one is left with the conclusion that the rate-determining step at low buffer concentrations is almost certainly the buffer-catalyzed dehydration of the carbinolamine **9** to quinolinate (**3**). The observed secondary deuterium isotope effect is consistent with this because the transition state for the dehydration reaction would have the relevant carbon hybridized somewhere between sp^3 and sp^2, i.e., more sp^3-like than the starting material **2**. Furthermore, similar secondary isotope effects have been observed for several other carbonyl group reactions.[19,23]

There is ample precedent for buffer catalysais of carbinolamine dehydration[24] as proposed in the **9** to **3** conversion. Although the mechanisms of intramolecular Schiff base formation have not been examined in great detail, bimolecular reactions of this type occur by rate-limiting acid-catalyzed dehydration of a carbinolamine addition intermediate at neutral and basic pH values and often show a range of pH values where the reaction velocity is independent of pH (a water-catalyzed reaction). The dehydration usually is catalyzed by buffer acids and more rarely by buffer bases. Base catalysis of dehydration can occur when less basic amines are used for Schiff base formation as is the case here.

The characteristic bell-shaped pH-rate profile, and the attendant decreasing rate with increasing acidity that is found for numerous bimolecular Schiff base forming reactions, is not seen in the kinetics of quinolinic acid formation from **2**, but that is expected because of the low pK_a of the conjugate acid of the vinylogous amide group. Furthermore, in the present case, protonation of a carboxylate group of **2** (pK_a = 5.0) and the proton-catalyzed reaction seen below pH 4 are providing alternate kinetic pathways which prevent such kinetics being observed.

Although intramolecular Schiff base formation has received little attention, the intramolecular aminolysis of esters has been extensively studied[24,25] and is known to occur by rate-limiting breakdown of a tetrahedral intermediate. For such reactions, concerted general acid catalysis of alcohol elimination has been demonstrated as well as a buffer dependent change in the rate-determining step.[26] Clearly some differences exist between the mechanism for aminolysis and Schiff base formation, but the many similarities of these two intramolecular reactions add credence to the present interpretation of the buffer catalysis.

Whether the slow step at high buffer concentration is the conversion of **6** to **7** or **8** to **9** remains to be considered. For several reasons it is more likely to be the pericyclic **8** to **9** conversion rather than the **6** to **7** step. Perhaps the strongest argument against the latter is that, because **6** has so much resonance stabilization (it is a vinylogous amide), one would expect that the **7** to **6** reverse reaction would be very rapid, thus requiring enforced buffer catalysis[21,22] if the reaction proceeded through **7** as an intermediate. However, as discussed above, enforced buffer catalysis of the reaction at low buffer concentrations is not observed. Another argument, through a relatively weak one, against the **6** to **7** step being rate determining at high buffer is that a negligible D_2O effect is observed, and the formation of such a zwitterion would be expected to show at least a small solvent isotope effect.[27,28]

In addition to arguments against the **6** to **7** step being the slow one at high buffer, there are several positive indications that the pericyclic **8** to **9** ring closure is the rate-determining step under such conditions. Thus, the lack of buffer catalysis, lack of any D_2O effect, and the observance of a secondary deuterium isotope effect[29] are what would be expected for such a mechanism. Furthermore, the rapid base catalyzed conversion of **2** to **3** at pH values greater than 11 is readily understandable if a pericyclic ring closure is occurring. At high pH the vinylogous amide **2** would be expected to ionize to the anion, and pericyclic ring closures of related anions are known to proceed much more rapidly than in the case of the neutral species.[30] It seems likely that **3** formation at the plateau region from pH 4–5 (Figure 1) may be occurring by a similar pericyclic ring closure of a protonated (on a carboxyl group) form of **2**, but insufficient data were obtained to warrant extensive speculations concerning the mechanism in this pH region.

Control of Quinolinate and Nicotinamide Biosynthesis in Vivo. If the **2** to quinolinate conversion is nonenzymic in vivo, as all current evidence indicates, then the present results clarify to some extent how biological systems probably control the flux to quinolinate and the nicotinamide coenzymes. Under physiological conditions (37 °C, pH 7.4, high buffer and ionic strength), the half-time for the **2** to **3** conversion is approximately 6 min. Furthermore, this is essentially invariant with any small changes in the buffer or salt environment because the slow step is the pericyclic ring closure of **8** to **9**. With this reaction proceeding at such a constant rate, the amount of quinolinate formed will then depend only on the rate at which **2** is formed and on the rate at which it is converted to **4**, catalyzed by the decarboxylase (see Scheme I). Thus, although it is unusual to have a nonenzymic step at a branchpoint of such an important pathway, it is perhaps not too unreasonable when so little affects the reaction as in the present case. There is considerable evidence that the physiological activities of both the decarboxylase[4,31] and tryptophan-2,3-dioxygenase,[4,32] the first enzyme in the biosynthesis of **2** from tryptophan, are under strict dietary and hormonal control. Consequently, even though it is formed in a nonenzymic step, the flux to quinolinate can be precisely controlled by modifications of these other enzymes.

Conclusion

The data presented here indicate that, in the conversion of **2** to quinolinate, geometric isomerism of **2** to **6** is rapid and is never kinetically significant. At neutral pH, two different steps in the conversion of **6** to quinolinate (**3**) can be rate determining depending on the conditions. At low buffer concentrations the dehydration of a carbinolamine adduct is the slow step while, at high buffer concentrations, another step, believed to be a pericyclic ring closure, becomes rate determining. Under physiological conditions, this latter step will be rate determining because of the presence of numerous general acids and bases in the cell milieu. Since very little affects the rate of this reaction, the control of

(22) Eigen, M. *Angew. Chem., Int. Ed. Engl.* **1964**, *3*, 1–72. Jencks, W. P. *Acc. Chem. Res.* **1976**, *9*, 425–432.
(23) do Amaral, L.; Bull, H. G.; Cordes, E. H. *J. Am. Chem. Soc.* **1972**, *94*, 7579–7580.
(24) Jencks, W. P. *Catalysis in Chemistry and Enzymology*; McGraw-Hill: New York, 1969.
(25) Bruice, T. C.; Sturtevant, J. M. *J. Am. Chem. Soc.* **1959**, *81*, 2860–2870. Fife, T. H.; DeMark, B. R. *J. Am. Chem. Soc.* **1979**, *101*, 7379–7385. Kirby, A. J.; Mujahid, T. G.; Camilleri, P. *J. Chem. Soc., Perkin Trans. 2* **1979**, 1610–1616.
(26) Fife, T. H.; Duddy, N. W. *J. Am. Chem. Soc.* **1983**, *105*, 74–79.
(27) The solvolysis of *tert*-butyl chloride, which involves the conversion of a neutral reactant to a partially zwitterionic transition state as in the putative **6** to **7** conversion, goes 25–30% more slowly in D_2O than in H_2O (Laughton, P. M.; Robertson, R. E. *Can. J. Chem.* **1956**, *34*, 1714–1718).
(28) a reviewer has pointed out that if our conclusions are correct that the conversion of **8** to **9** and **9** to **3** are the only kinetically significant steps in the overall reaction, then there is no evidence that **6** is an obligatory intermediate. This point is well taken. However, one expects that it would be present as part of the equilibrium mixture that is the reactant, because the results require **8** to be in equilibrium with **2**, and thus it would almost certainly be in equilibrium with **6** as well.
(29) Humski, K.; Malojcic, R.; Borvic, S.; Sunko, D. E. *J. Am. Chem. Soc.* **1970**, *92*, 6534–6538.
(30) Evans, D. A.; Golub, A. M. *J. Am. Chem. Soc.* **1975**, *97*, 4765–4766. Carpenter, B. K. *Tetrahedron* **1978**, *34*, 1877–1884.
(31) Mehler, A. H.; McDaniel, E. G.; Hundley, J. M. *J. Biol. Chem.* **1958**, *232*, 323–330, 330–335.
(32) Schimke, R. T. *Adv. Enzymol.* **1973**, *37*, 135–187.

quinolinate and nicotinamide formation can thus be precisely controlled by modifications of the enzymes involved in the biosynthesis of **2** and in the metabolism of **2** by another pathway. Thus, although it is unusual to have a nonenzymic step compete with an enzymic one at a branchpoint in an important metabolic pathway, it is perhaps not too surprising since effective control, even of the products of the nonenzymic reaction, can still be achieved.

The Hydrated Potassium Complex of the Ionophore Monensin A

Walter Pangborn,* William Duax, and David Langs

Contribution from the Medical Foundation of Buffalo, Inc., Buffalo, New York 14203.
Received July 7, 1986

Abstract: The crystal structure of the potassium monensin A dihydrate has been determined (orthohombic, space group $P2_12_12_1$, a = 16.485 (2) Å, b = 19.189 (2) Å, c = 12.661 (1) Å, Z = 4). Examination of the conformation of the K^+ complex compared with that of the previously reported structures of several complexes, particularly the Na^+ complexes, reveals several features which correlate with the observed selectivity of monensin for Na^+ over K^+. Coordination of the K^+ ion involves changes in the conformation of a spiro-fused ring, the conformation of which is highly conserved in the structures of several Na^+ complexes. Preliminary molecular mechanics calculations are consistent with the conclusion that the coordination of the K^+ ion involves a distortion of the spiro-fused ring from its low-energy conformation. Furthermore, the coordination of the K^+ ion is less uniform than that observed in the Na^+ complexes.

The antibiotic monensin A (Figure 1) is a biologically active compound produced by a strain of *Streptomyces cinnamonensis*. A member of the family of monocarboxylic acid, polycyclic, polyether antibiotics, it induces monovalent cation permeability, exhibits selectivity for Na^+ over K^+, and has a greater stability constant with Na^+ than K^+.[1]

The selectivity of ionophores must be largely influenced by the relative binding energies of the various cations. Among the factors influencing this would be cation size, the distribution of ligands, and the conformational flexibility of the ionophore. However, the relative importance of the various parameters affecting selectivity is disputed. In order to attempt to relate structural features to the selectivity of ionophores, the structures of the free acid should be compared with those of the complexes of at least two cations with different selectivities.

Monensin is one of the ionophores for which the most crystallographic data are available. For monensin A, the structures of the free acid,[2] the hydrated and anhydrous forms of Na^+ complex,[3] the NaBr complex,[4] and the hydrated Ag^+ complex[5] have been determined. Also, the monohydrate of the Na^+ complex of monensin B,[6] and the Li^+ and Ag^+ salts of monensin B,[7] which differs from monensin A by the replacement of an ethyl group by a methyl group, have been determined. The crystal structure of the dihydrate of the K^+ complex of monensin A reported here provides the data required to compare the structures of the complexes of monensin A with cations with which it exhibits selectivity.

Experimental Section

Single crystals of the dihydrate of the potassium complex of monensin A, $C_{36}H_{61}O_{11}K\cdot 2H_2O$, were grown from an ethanol/water solution. These crystals are isomorphous with previously reported dihydrate sodium and silver complexes of monensin A ($P2_12_12_1$, a = 16.485 (2) Å, b = 19.189 (2) Å, c = 12.661 (1) Å, V = 4005 Å^3, Z = 4, ρ_c = 1.24 g cm^{-3}). A single crystal (0.4 × 0.8 × 0.8 mm) was mounted and a total of 4610 independent data ($\sin\theta_{max}/\lambda$ = 0.61) were collected on an Enraf-Nonius CAD-4 diffractometer with use of nickel-filtered copper radiation. Intensities were corrected for Lorentz and polarization factors but not for extinction or absorption (μ(Cu Kα) = 16.5 cm^{-1}). Of the 4610 measured data, 4499 were considered observed on the basis of $I > 2\sigma I$. The variance of each F was calculated according to the method of Stout and Jensen[8] with an instability correction of 0.04. Unobserved data were given zero weight.

The starting coordinates were those reported for the isomorphous hydrated sodium complex.[3] The structure was refined by full matrix least squares, minimizing $\sum w(|F_o| - |F_c|)^2$, treating all non-hydrogen atoms anisotropically. In the final cycles of refinement, hydrogen atoms, except for those of hydroxyl groups, were included at calculated positions. The refinement converged to a final residual of 0.046 and a weighted residual of 0.068. Positional parameters appear in Table I.

Results and Discussion

Superficially, all the cation complexes of monensin A are similar. In the K^+ complex, as in other complexes, two intramolecular hydrogen bonds involving the carboxyl oxygens and two hydroxy groups at the opposite end of the molecule are found. These head-to-tail hydrogen bonds (O(1)–O(11) = 2.51 Å and O(2)–O(10) = 2.62 Å), common in this class of antibiotics, produce a pseudocyclic conformation which serves to form the cavity in which the cation is coordinated. This intramolecular hydrogen bonding and cation coordination are illustrated in Figure 2. Bond lengths and angles are illustrated in Figure 3. The crystal packing and intermolecular hydrogen bonding found here are similar to that reported in the hydrated Na^+ complex.

All hydrogen bond distances are listed in Table II. In addition to a hydrogen bond between the two independent water molecules, each water is involved in two hydrogen bonds to the ionophore. As in the hydrated Na complex, there is an ionophore water layer perpendicular to the y axis. Adjacent layers are related by the screw axis parallel to y. There are no hydrogen bonds between layers.

(1) Dobler, M. *Ionophores and Their Structures*; Wiley-Interscience: New York, 1981; pp 16, 20, 77–83.
(2) Lutz, W. K.; Winkler, F. K.; Dunitz, J. D. *Helv. Chim. Acta* **1971**, *54*, 1103.
(3) Duax, W. L.; Smith, G. D.; Strong, P. D. *J. Am. Chem. Soc.* **1980**, *102*, 6725.
(4) Ward, D. L.; Wei, K. T.; Hoogerheide, J. C.; Popov, A. I. *Acta Crystallogr., Sect. B* **1978**, *B34*, 110.
(5) Pinkerton, M.; Steinrauf, L. K. *J. Mol. Biol.* **1970**, *49*, 533.
(6) Barrans, P. Y.; Alleume, M.; Jeminet, G. *Acta Crystallogr., Sect B* **1982**, *B38*, 1144.
(7) Walba, D. M.; Hermsmeir, M.; Haltiwanger, R. C.; Noordik, J. H. *J. Org. Chem.* **1986**, *51*, 245.
(8) Stout, G. H.; Jensen, L. H. *X-Ray Structure Determinations*; Macmillan: New York, 1968; p 457.

0002-7863/87/1509-2163$01.50/0